

# Fast Optimization of Array Antenna Enclosed by Asymmetric Radome Using AEP Combined with Enhanced HGAPSO

Legen Dai, Yongjun Xie, Chungang Zhang, and Peiyu Wu\*

**Abstract**—An efficient analysis and optimization method is proposed to compensate the influence of asymmetric radome on an antenna by correcting amplitude and phase of the excitations. The asymmetrical and heteromorphic radomes are inevitable for the radar on high-speed aircraft. Many previous researches focused on the optimization of the radome structure and thickness to reduce the influence of radomes. However, the influence of complex streamlined radome cannot be compensated by merely optimizing the structure and thickness of the radome. Therefore, an alternative optimization method, optimizing amplitude and phase of feeds, is used in this paper. This paper adopts the active element pattern (AEP) technique, utilizing full-wave simulation method to extract the AEP for each antenna element and computing radiation patterns of array antenna by using vector composition of AEP. In combination with hybrid genetic algorithm-particle swarm optimization (HGAPSO), the antenna radiation characteristics can be obtained by updating excitations, which avoid the repeated full-wave simulation in the optimization process. Furthermore, the speed updating formula of PSO algorithm is improved combined with prior information, and the convergence speed is further increased. Finally, a 64 elements array antenna-radome system was optimized as an example in the cases of continuously adjustable phase and digital discrete phase.

## 1. INTRODUCTION

The airborne radomes of high-speed aircraft are invariably subject to high aerodynamic stresses and therefore, have to be streamlined, which tend to severely degrade the electromagnetic (EM) performance. The degradations of EM performance would seriously affect the direction finding and cruising characteristics of the radar on high speed aircraft. Boresight error (BSE), transmission loss (TL) and null depth (ND), the three important EM characteristics of radome-enclosed antenna, need to be optimized [1].

The problem of determining the radiation characteristics of radome-closed antennas has been addressed by a number of researchers employing a variety of different approaches. Orta et al. analyzed the radiation characteristics of dielectric radome covered antennas by ray techniques combined with reciprocity theorem [2]. Chikaoka et al. determined the influences of scattered waves caused by metal frames of a radome by using geometrical theory of diffraction (GTD) [3]. Grodon and Mittra used finite element method (FEM) to analyze the array antenna with axisymmetric inhomogeneous dielectric radome [4]. With radome structures becoming more and more complex due to their practical purposes, it is very difficult to compute and analyze radome-enclosed antennas. Although full-wave simulation method can be used, the computing time may be extremely long. It is well known that optimization algorithms need plenty of iterations, and thus directly using the full-wave simulation in each step may take a very long time. Especially for electrically large radome, the time consumption is unacceptable.

---

*Received 13 May 2021, Accepted 11 July 2021, Scheduled 19 July 2021*

\* Corresponding author: Peiyu Wu (wupuuu@yahoo.com).

The authors are with the School of Electronic and Information Engineering, Beihang University, Beijing 100191, China.

To guarantee the proper functioning of radome-enclosed antennas, previous researches focused on the optimal design of radomes. Hsu et al. systematically proposed the concept of designing radome thickness profile to improve the EM performance [5, 6], where the thickness profile was parameterized via B-spline representation, and simulated annealing technique was employed to optimize the BSE. Nair and Jha proposed a novel A-sandwich radome design based on optimum power reflection, and then this method was extended to monolithic half-wave wall design [7, 8]. Xu et al. used multi-objective particle swarm optimization algorithm to optimize the thickness of radome wall, which can reduce the BSE and TL simultaneously for airborne radomes [9]. The optimization objective of these methods was to find the optimal thickness distribution of the radome, and thereby improve the EM performance for radome-enclosed antenna. However, these methods would not be applicable when the radome must be a specific streamlined structure to meet the requirements of the environment and strength of the high-speed aircraft.

Active element pattern (AEP) is a method to predict the scan performance of large phased array antennas, which was first introduced by Pozar in 1994 [10] and widely used in the analysis of phased array antenna. Ou Yang et al. obtained the AEP of conformal phased array by measurement and optimized the element excitations combined with improved NSGA-II algorithm [11]. He et al. [12] and Yang et al. [13] analyzed the radiation characteristics of conformal antenna arrays with the use of the AEP technique. Besides, the effectiveness and advantage of AEP method were proved by comparing with full-wave simulation in these two papers. According to the discussion of the two paragraphs above, the previous works have limitations in the analyzation and optimization of the large asymmetric radomes. As an accurate analytical method, the AEP method may solve the problem that the analyzation needs too long time. In combination with the optimization for the amplitude and phase of each element, the radiation characteristics of the radome-enclosed antenna might be corrected. In this proposed method, the full-wave simulation needs to be solved only once to get the AEP of each element, then the new radiation patterns of the array antenna are obtained by rapid combination of the AEP and the optimized feeds.

The genetic algorithm (GA) and particle swarm optimization (PSO) algorithm are on the rise in electromagnetics as design tools and problem solvers because of their versatility and ability to optimize in complex multimodal search spaces [14–16]. PSO algorithm is a kind of bionic algorithms and originates from the research of the predation of birds, with characteristics of easy implementation, high precision, and fast convergence. However, the original PSO had difficulties in controlling the balance between exploration and exploitation because it tends to favor the intensification search around the better solutions previously found. In such a context, the PSO appears to be lacking global search ability [17]. The key genetic operators in GA, namely selection, crossover, and mutation may compensate this shortage. Consequently, the hybrid algorithms which attempt to combine the advantages of different algorithms are proposed and widely used in complex optimization problem. Liu et al. used a hybrid PSO-GA algorithm to solve the job shop scheduling problem in machine tool production [18]. Zhang et al. compared the hybrid PSO-GA and basic GA in the optimization of biodiesel engine performance and proved the efficiency of the hybrid PSO-GA [19]. Based on these reasons, an enhanced hybrid genetic algorithm-particle swarm optimization (HGAPSO) is proposed in this article. In the proposed HGAPSO algorithm, the genetic operators such as crossover and mutation operators in GA are used to update the particles in the PSO algorithm, which combined the merits from both the GA and PSO algorithm. Moreover, the initial amplitude and phase of the elements can be estimated according to the initial error, the optimization algorithm is enhanced by improving the speed updating formula of HGAPSO algorithm.

In this paper, AEP is used to quickly obtain the radiation characteristics of array antenna with asymmetric radome. And the feeds of array antenna are improved by the enhanced HGAPSO efficiently. First, the correction problem for radome-enclosed antenna is discussed, and the general approach which aimed to optimize the amplitude and phase of elements excitation is then established. Second, an introduction of AEP method is made, and the enhanced HGAPSO algorithm is explained. Then the array antenna with axi-asymmetric radome is employed as an example for optimization. The improvement of radiation characteristics for array antenna and the comparison of optimization efficiency are provided at last.

## 2. METHODOLOGY

### 2.1. Problem Specification

As shown in Fig. 1, when a plane wave is irradiated on a radome, the wave will be refracted, reflected, scattered, and attenuated, and the surface wave or guided waves will be stimulated on the surface of the radome, which means that the field on the antenna is composed of multiple components. Whether the radome-enclosed antenna is in the receiving state or the emission state, the radome introduces an inhomogeneous insertion phase delay to the incident/radiation wave of the antenna and introduces modulation to the amplitude of the transmission coefficient. As a result, the main lobe width, beam pointing deviation, and gain loss of sum beam pattern will be induced. Besides, the difference beam pattern is also affected such as null point offset and null depth level elevated. Generally, the radome will affect the BSE, TL, and ND of the array antenna.

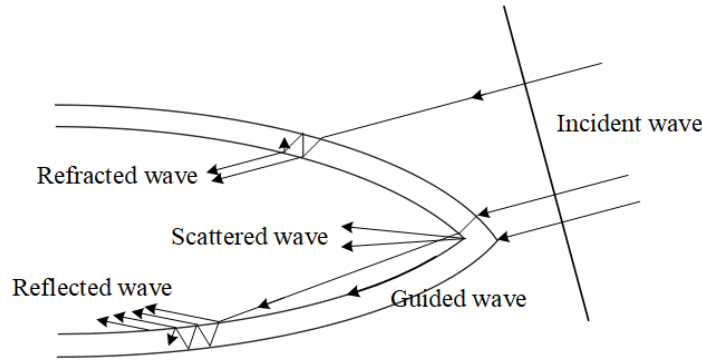


**Figure 1.** The sketch picture of waves in the radome.

As the parameters of the radome material and structure have been established, the BSE, TL, and ND of the radome-enclosed antenna can be expressed as

$$\text{BSE} = \text{BSE}(X_a, X_\phi, \alpha, f) \tag{1}$$

$$\text{TL} = \text{TL}(X_a, X_\phi, \alpha, f) \tag{2}$$

$$\text{ND} = \text{ND}(X_a, X_\phi, \alpha, f) \tag{3}$$

where  $X_a$  is the amplitude of array element,  $X_\phi$  the phase of array element,  $\alpha$  the beam direction, and  $f$  the frequency of antenna.

The optimization problem is to find the minimum value of  $F(\Phi)$ .  $\Phi = (X_a, X_\phi, \alpha)$  when the frequency of array antenna is determined.

$$\begin{cases} \min F(\Phi) = w_1 \text{BSE}(\Phi) + w_2 \text{TL}(\Phi) - w_3 \text{ND}(\Phi) \\ \text{BSE} \leq \text{BSE}_{\max}, \text{TL} \leq \text{TL}_{\max}, \text{ND} \geq \text{ND}_{\min} \\ X_a = [A_1, A_2, \dots, A_N]^T, X_\phi = [\phi_1, \phi_2, \dots, \phi_N]^T \\ |\alpha| \leq \alpha_m, |A_n - A_n^0| \leq \varepsilon_a, |\phi_n - \phi_n^0| \leq \varepsilon_\phi \end{cases} \tag{4}$$

where  $A_n$  and  $\phi_n$  are the amplitude and phase of the  $n$ th element;  $A_n^0$  and  $\phi_n^0$  are the initial values of  $A_n$  and  $\phi_n$ ;  $\varepsilon_a$  and  $\varepsilon_\phi$  are the limits of the range of  $A_n$  and  $\phi_n$ ;  $\alpha_m$  is the maximum scan angle of the array antenna.

Figure 2 shows the correction process for array antenna with radome. The relationship between EM performance and element excitation is obtained by full-wave simulation and AEP synthesis. Through rapid optimization by HGAPSO for the element's excitation amplitude and phase, the EM performance of array antenna with radome can be quickly improved.

### 2.2. Calculating the Radiation Characteristics by AEP

Full-wave simulation can be used to obtain the radiation characteristics for any array antenna with an arbitrary shape radome, while it takes too long to use the full-wave simulation directly in the process

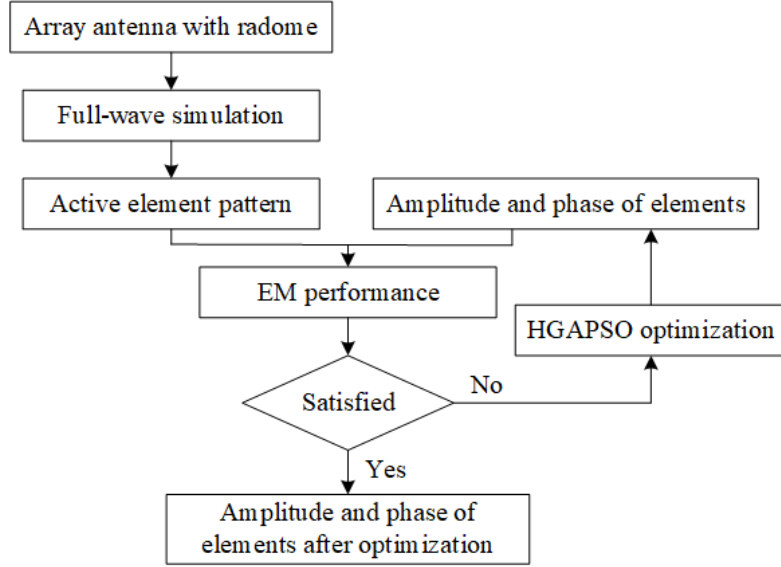


**Figure 2.** Correction process for array antenna with radome.

of optimization. Thus, the AEP technique is used for the fast calculation of an array antenna with radome.

The AEPs for the array enclosed by asymmetric radome are obtained by full-wave simulation. First, the array antenna with radome is analyzed by full wave simulation. The results include the mutual coupling between antenna elements and the influence of radome. Next, exciting each element separately, the AEP of the active element could be extracted. Thus, the AEPs of all  $N$  elements could be obtained by once full-wave simulation and  $N$  times post-processing. Then the pattern of array antenna with radome can be calculated as

$$F(\theta, \varphi) = \sum_{n=1}^N \sqrt{A_n} \cdot \text{mag}_n(\theta, \varphi) \cdot e^{j \cdot [\text{ang}_n(\theta, \varphi) + \phi_n]} \quad (5)$$

where  $\text{mag}_n(\theta, \varphi)$  and  $\text{ang}_n(\theta, \varphi)$  are the magnitude pattern and phase pattern for the  $n$ th element in array antenna;  $A_n$  is the excitation amplitude for the  $n$ th element;  $\phi_n$  is the excitation phase for the  $n$ th element.

As shown in Eq. (5), the pattern of an array antenna with any excitation can be obtained by the vector composition of the AEPs if the AEP for each element is obtained. The full-wave simulation needs to be solved only once, and the new radiation pattern of the antenna array is obtained by rapid combination of the AEP. Accordingly, the calculation of the AEP for each element does not significantly increase the computation, and the optimization efficiency would be greatly enhanced.

### 2.3. Enhanced HGAPSO Algorithm

In the general PSO model, the position and velocity of a particle at the current iteration,  $X(i)$  and  $V(i)$ , respectively, can be updated as

$$V(i+1) = w \cdot V(i) + c_1 \cdot r_1 [pbest(i) - X(i)] + c_2 \cdot r_2 [gbest(i) - X(i)] \quad (6)$$

$$X(i+1) = X(i) + V(i+1) \quad (7)$$

where  $i$  is the current iteration,  $i+1$  the next iteration, and  $w$  is the inertia weight and is used to reduce the current velocity or the impact of the previous velocity. Two weight parameters,  $c_1$  (individual interest factor) and  $c_2$  (social interest factor), are used to balance the individual and social confidence factors for the particle.  $r_1$  and  $r_2$  are two random numbers between 0 and 1 to enrich the search space.  $pbest$  is the particles local best, and  $gbest$  is the global best, i.e., the best among all the particles.

In application,  $X$  is a design variable, and its value is modified constantly by  $V$ . The modification considers the information of both the particle itself and its neighbors. Finally, an objective function must be given to evaluate the quality of a position. This behavior continues until a satisfaction criterion is reached.

When array antenna points to  $\alpha$ , the approximate solution of antenna excitation can be estimated according to the initial boresight error of the antenna. The existing velocity updating formula (6) can be improved by using the approximate solution *approx* as

$$V(i+1) = w \cdot V(i) + \sigma \cdot \{c_1 \cdot r_1 [pbest(i) - X(i)] + c_2 \cdot r_2 [gbest(i) - X(i)]\} + (1 - \sigma) \cdot r_3 \cdot [approx - X(i)] \tag{8}$$

where  $\sigma = \sqrt{i/i_{max}}$  is the weight parameters.  $\sigma$  is small, and the weight of the approximate solution is large in early iterations. Particles will move to the neighborhood of the approximate solution fast. The exact solution will be found quickly if it is in the area nearby. If the exact solution is not near the approximate solution, the value of  $\sigma$  will increase gradually with the raise of iteration times and tend to be 1. When the weight of the approximate solution is smaller to 0, Equation (8) degenerates into Eq. (6).

The present hybrid method in this paper is performed in a two-step process. A generation has  $N$  particles, and their values are evaluated. First, a ‘‘PSO update step’’ will be done on the best  $n$  particles and produce  $n$  offspring for use in the next generation.  $n$  is determined by multiplying the keep rate (that is  $n/N$ ) by the total number of variables. The rest  $N - n$  particles will be discarded to make room for the new offspring generated by the GA step. Second, in the GA step, genetic variants are taken by crossing over with the survived  $n$  PSO particles and dynamic mutation to generate  $N - n$  members. As a result, the new generation will have  $N$  particles whose values will be evaluated again. Overall, the hybrid method constructs a PSO-GA stepwise algorithm based on a PSO update step followed by a GA step. The flowchart showing the HGAPSO is presented in Fig. 3.

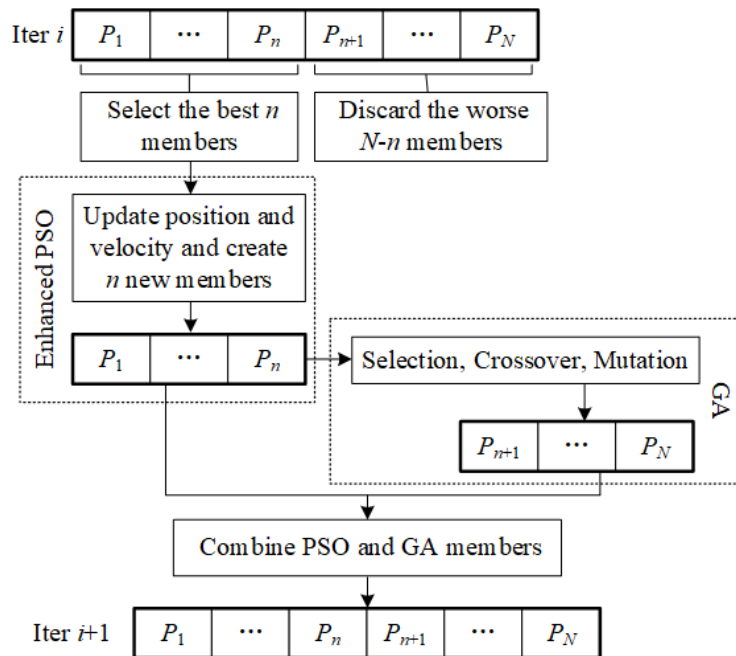
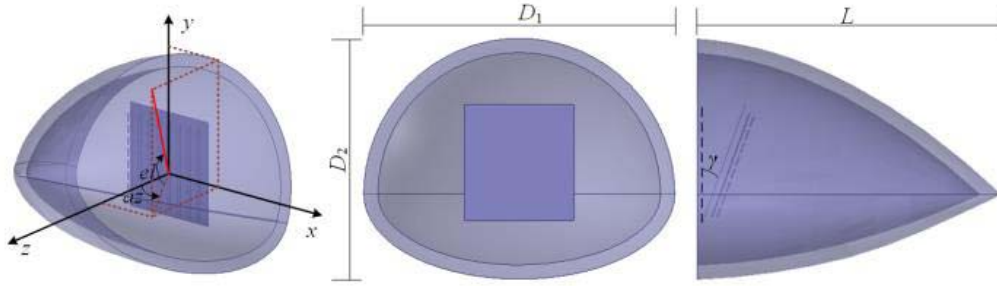


Figure 3. Flowchart of the enhanced HGAPSO algorithm.

### 3. OPTIMIZATION EXAMPLES

To illustrate the validity of the proposed method, an array antenna with asymmetric radome is optimized, as shown in Fig. 4. The height of the radome  $L$  is  $12.85\lambda$ ; the long axis ( $D1$ ) and minor



**Figure 4.** Model of array antenna with asymmetric radome.

axis ( $D2$ ) of bottom are  $11.73\lambda$  and  $9\lambda$ , respectively; the thickness is  $0.55\lambda$ . The dielectric constant of the radome is 3.1, and the loss tangent is 0.005. The array antenna has  $8 \times 8$  elements and works at 16 GHz. The angle between the array antenna and the bottom of radome  $\gamma$  is  $20^\circ$ . The “ $az$ ” and “ $el$ ” in Fig. 4 are azimuth angle and elevation angle, respectively. The optimized design specifications are as follows: the maximum gain is greater than 20 dB, and the null depth of difference beam is larger than 25 dB.

### 3.1. Comparison of Optimization Results

In the case that the amplitude and phase of elements excitation are continuously adjustable, the optimization results of BSE, when the antenna points to  $20^\circ$  in azimuth angle and scans from  $-50^\circ$  to  $50^\circ$  in elevation angle, are shown in Fig. 5. Figs. 5(a) and (b) are the BSEs of azimuth difference beam and elevation difference beam, respectively. It can be observed that the BSE values of all scanning angles are smaller than  $0.02^\circ$ , whereas the maximum BSE value before optimization is  $2.32^\circ$ .

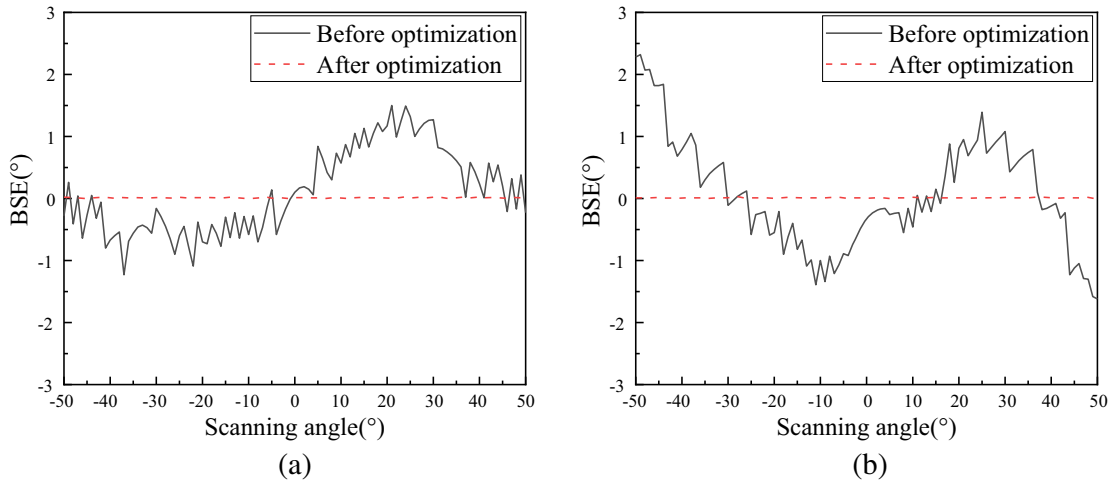


**Figure 5.** BSE values before and after optimization in the case that the amplitude and phase of antenna excitation are continuously adjustable: (a) azimuth difference beam and (b) elevation difference beam.

The patterns in the main lobe cut plane, when the antenna points to  $20^\circ$  in azimuth angle and  $30^\circ$  in elevation angle, are shown in Fig. 6. It is obvious that the BSE value decreases from  $1.07^\circ$  to  $0^\circ$  after optimization. Besides, the optimized maximum gain of the array antenna is 20.25 dB, and the null depth of difference beam is 26.30 dB, which meet the design requirements.

The above optimization results are based on the assumption that the phases of antenna elements are continuous adjustable. However, the digital phase shifter is usually used in the actual antenna array, which can only adjust the integer times of the minimum adjustment. A 6-bit digital phase shifter is

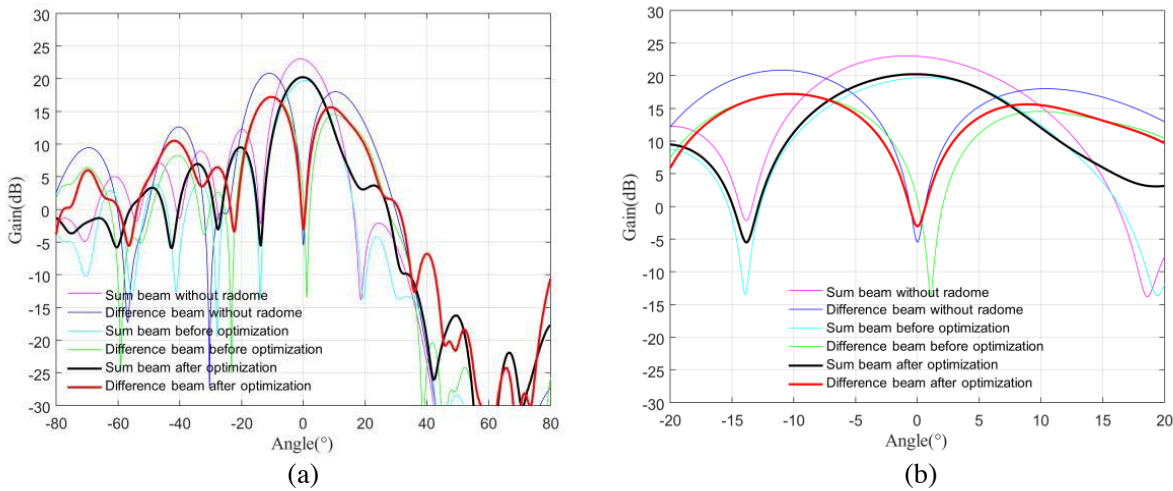


**Figure 6.** Patterns in the main lobe cut plane before and after optimization in the case that the amplitude and phase of antenna excitation are continuously adjustable: (a) angle range  $[-80, 80]$  and (b) angle range  $[-20, 20]$ .

taken as an example, in which case the minimum phase adjustment is 5.625 degrees. The initial phase of the array antenna is based on the round up and down method. When the remainder of phase divided by 5.625 is smaller than 0.5, the decimal fractions will be omitted, while all the others will be rounded up to 1. The optimization results of BSE, when the antenna points to  $20^\circ$  in azimuth angle and scans from  $-50^\circ$  to  $50^\circ$  in elevation angle, are shown in Fig. 7.

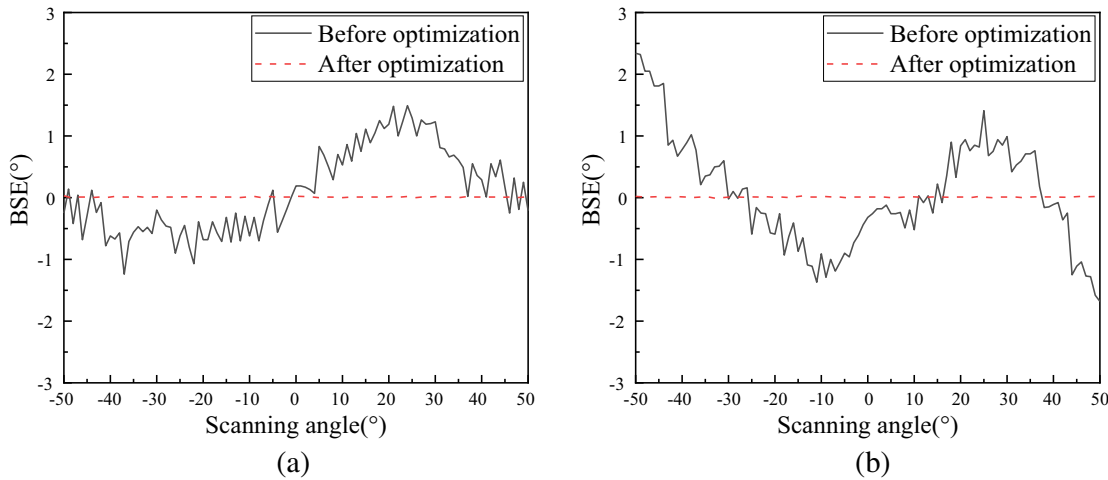


**Figure 7.** BSE values before and after optimization in the case that the excitations of antenna are digital discrete phase: (a) azimuth difference beam and (b) elevation difference beam.

Figures 7(a) and (b) are the BSEs of azimuth difference beam and elevation difference beam, respectively. It can be observed that the BSE values of all scanning angles are smaller than  $0.02^\circ$ , whereas the maximum BSE value before optimization is  $2.34^\circ$ .

The patterns in the main lobe cut plane, when the antenna points to  $20^\circ$  in azimuth angle and  $30^\circ$  in elevation angle, are shown in Fig. 8. It is obvious that the BSE value decreases from  $1.08^\circ$  to  $0^\circ$  after optimization. Besides, the optimized maximum gain of the array antenna is 20.14 dB, and the null depth of difference beam is 40.15 dB, which meet the design requirements. The amplitude and phase of partial elements for difference beam before and after optimization are listed in Table 1.

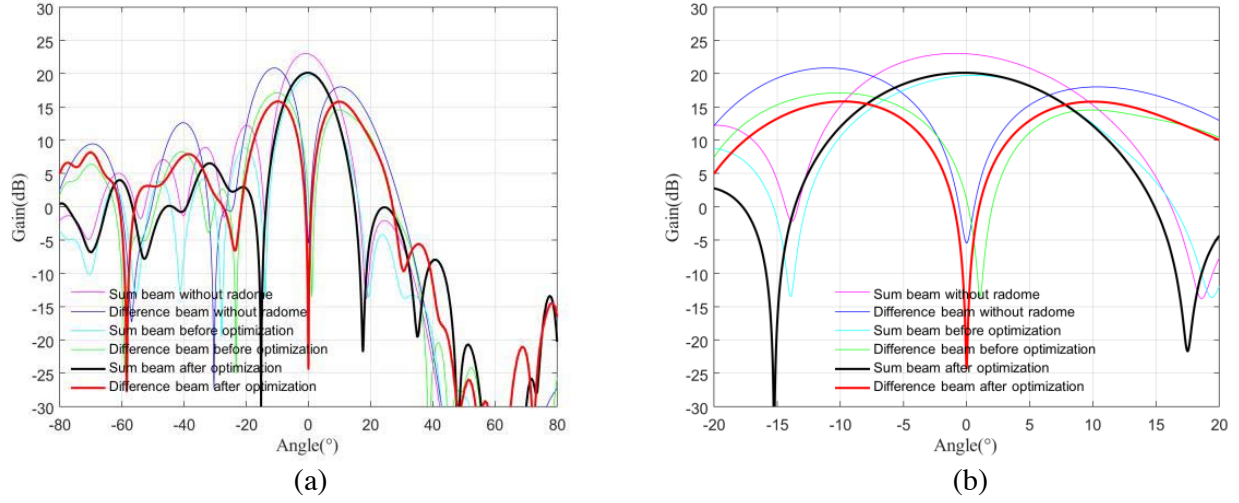


**Figure 8.** Patterns in the main lobe cut plane before and after optimization in the case that the excitations of antenna are digital discrete phase: (a) angle range  $[-80, 80]$  and (b) angle range  $[-20, 20]$ .

**Table 1.** Excitations of the antenna array before and after optimization.

No.	Initial Amplitude (V)	Initial Phase (°)	Optimized Amplitude (V)	Optimized Phase (°)
1	1	163.125	1.35	73.125
2	1	106.875	0.89	28.125
3	1	50.625	0.77	118.125
4	1	354.375	0.85	39.375
5	1	298.125	0.79	326.25
6	1	241.875	0.82	196.875
7	1	185.625	1.19	225
8	1	129.375	1.26	168.75
...	...	...	...	...
57	1	50.625	0.71	73.125
58	1	5.625	1.11	5.625
59	1	61.875	0.97	95.625
60	1	118.125	0.69	50.625
61	1	174.375	1.35	157.5
62	1	230.625	1.25	292.5
63	1	286.875	0.88	225
64	1	343.125	0.66	382.5

### 3.2. Comparison of Optimization Efficiency

Figure 9 shows the best fitness values of the objective function using basic GA, PSO, HGAPSO, and enhanced HGAPSO, respectively. The population number is 64, and the maximum iteration number is 100. The antenna points to  $20^\circ$  in azimuth angle and  $30^\circ$  in elevation angle. It is clearly shown that, compared with basic GA and PSO algorithm, HGAPSO has faster convergence speed and higher convergence accuracy. In addition, the convergence speed and accuracy of HGAPSO are further

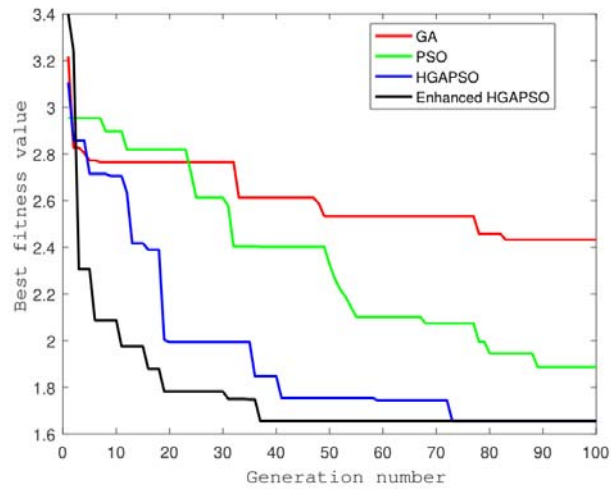


**Figure 9.** Best fitness values of the objective function using basic GA, PSO, HGAPSO and enhanced HGAPSO respectively.

improved by adding the priori information.

Table 2 gives the optimization time for HGAPSO combined with AEP or not. The optimized parameters and objective function are the same, and the optimization process is performed on a PC with i7 CPU and 32 GB memory. In the circumstance of  $20^\circ$  in azimuth angle, 101 points need to be optimized between  $-50^\circ$  and  $50^\circ$  in elevation angle, which need to optimize 101 points in all. The total optimization time, using the post-processing module of numerical simulation software directly, is 762911 seconds. By contrast, the optimization time using AEP synthesis method is 7549 seconds. Furthermore, the processing time for numerical simulation software will increase when the radome-enclosed antenna is larger, while the computing time for AEP synthesis will remain unchanged.

**Table 2.** Optimization time for HGAPSO which combined with AEP or not.

	Total time for 101 points (s)	Average time for single point (s)
Without AEP	762911	7554
With AEP	7549	75

In conclusion, the optimization method proposed in this paper can greatly improve the optimization efficiency. There are mainly three improvements as follows. Firstly, the analytic method is used to solve the array pattern in the optimization iteration process, which greatly improves the solving speed. Secondly, PSO algorithm is added to update the selected particles in the selection step of traditional GA, which improves the convergence speed of the optimization algorithm. Finally, the prior information is added to the PSO velocity update formula. When the optimal solution is in the near field of the estimated value, the algorithm can find the optimal solution quickly.

#### 4. CONCLUSION

In this paper, a new method, which is based on the AEP technique and combined with the enhanced HGAPSO, is proposed to solve the optimization problem of array antennas with asymmetric radomes. Compared with the traditional radome-enclosed antenna optimization method, the proposed method gives a new way to optimize antennas with arbitrary shape radomes. The optimization results show that the BSE of radome-enclosed antennas can be reduced or even eliminated by optimizing the excitation

amplitude and phase, no matter what the amplitude and phase of elements excitation are continuously adjustable or digital discrete adjustable. Compared with the basic GA and PSO algorithm, HGAPSO can converge faster to the optimal solution. By using the approximate solution to improve the velocity updating formula of PSO algorithm, the optimization efficiency accelerates even further. By using the AEP technique, a large number of repeated computations are avoided in the process of optimization, which greatly accelerates the optimization.

## ACKNOWLEDGMENT

This work is supported by the National Natural Science Foundation of China (61571022, 61971022) and National Key Laboratory Foundation of China (HTKJ2019KL504013, 61424020305).

## REFERENCES

1. Kozakoff, D. J., *Analysis of Radome-enclosed Antennas*, 2nd Edition, Artech House, Norwood, MA, USA, 2010.
2. Orta, R., R. Tascone, and T. Zich, "Performance degradation of dielectric radome covered antennas," *IEEE Trans. Antennas Propagat.*, Vol. 36, No. 12, 1707–1713, 1988.
3. Chikaoka, S., I. Chiba, Y. Sunahara, and T. Numazaki, "Pattern synthesis of an array antenna in a radome," *Antennas and Propagation Society International Symposium, 1990, AP-S, Merging Technologies for the 90's, Digest*, 852–855, IEEE, 1990.
4. Gordon, R. K. and R. Mittra, "Finite element analysis of axisymmetric radomes," *IEEE Trans. Antennas Propagat.*, Vol. 41, No. 7, 975–981, 1993.
5. Hsu, F., P. R. Chang, and K. K. Chan, "Optimization of two-dimensional radome boresight error performance using simulated annealing technique," *IEEE Trans. Antennas Propagat.*, Vol. 41, No. 9, 1195–1203, 1993.
6. Hsu, F., K. K. Chan, P. R. Chang, and S. H. Chao, "Optimal boresight error design of radomes of revolving symmetry," *Electron. Lett.*, Vol. 30, No. 19, 1561–1562, 1994.
7. Nair, R. U. and R. M. Jha, "Novel A-sandwich radome design for airborne applications," *Electron. Lett.*, Vol. 43, No. 15, 787–788, 2007.
8. Nair, R. U. and R. M. Jha, "Electromagnetic performance analysis of a novel monolithic radome for airborne applications," *IEEE Trans. Antennas Propagat.*, Vol. 57, No. 11, 3664–3668, Nov. 2009.
9. Xu, W. Y., B. Y. Duan, P. Li, N. G. Hu, and Y. Y. Qiu, "Multiobjective particle swarm optimization of boresight error and transmission loss for airborne radomes," *IEEE Trans. Antennas Propagat.*, Vol. 62, No. 11, 5880–5885, 2014.
10. Pozar, D. M., "The active element pattern," *IEEE Trans. Antennas Propagat.*, Vol. 42, No. 8, 1176–1178, 1994.
11. Ou Yang, J., Q. R. Yuan, F. Yang, H. J. Zhou, Z. P. Nie, and Z. Q. Zhao, "Synthesis of conformal phased array with improved NSGA-II algorithm," *IEEE Trans. Antennas Propagat.*, Vol. 57, No. 12, 4006–4009, 2009.
12. He, Q. Q., B. Z. Wang, and W. Shao, "Radiation pattern calculation for arbitrary conformal arrays that include mutual-coupling effects," *IEEE Antennas Propag. Mag.*, Vol. 52, No. 2, 57–63, 2010.
13. Yang, X. S., H. Qian, B. Z. Wang, and S. Q. Xiao, "Radiation pattern computation of pyramidal conformal antenna array with active-element pattern technique," *IEEE Antennas Propag. Mag.*, Vol. 53, No. 1, 28–37, 2011.
14. Weile, D. S. and E. Michielssen, "Genetic algorithm optimization applied to electromagnetics: A review," *IEEE Trans. Antennas Propagat.*, Vol. 45, No. 3, 343–353, 1997.
15. Robinson, J. and Y. Rahmat-Samii, "Particle swarm optimization in electromagnetics," *IEEE Trans. Antennas Propagat.*, Vol. 52, No. 2, 397–407, 2004.
16. Ho, S. L., S. Y. Yang, G. Z. Ni, E. W. C. Lo, and H. C. Wong, "A particle swarm optimization-based method for multiobjective design optimizations," *IEEE Trans. Magn.*, Vol. 41, No. 5, 1756–1759, 2005.

17. Ho, S. L., S. Y. Yang, G. Z. Ni, and H. C. Wong, "A particle swarm optimization method with enhanced global search ability for design optimizations of electromagnetic devices," *IEEE Trans. Magn.*, Vol. 42, No. 4, 1107–1110, 2006.
18. Liu, L. L., R. S. Hu, X. P. Hu, G. P. Zhao, and S. Wang, "A hybrid PSO-GA algorithm for job shop scheduling in machine tool production," *Inter. J. of Product. Resear.*, Vol. 53, No. 19, 5755–5781, 2015.
19. Zhang, Q., R. M. Ogren, and S. C. Kong, "A comparative study of biodiesel engine performance optimization using enhanced hybrid PSO-GA and basic GA," *Applied Energy*, Vol. 165, 676–684, 2016.